Finite element analysis of natural convective heat transfer in a porous square cavity filled with nanofluids in the presence of thermal radiation

Balla Chandra Shekar[1] **and Naikoti Kishan**[2]

Department of Mathematics, Osmania University, Hyderabad, Telangana State, India.

E-mails: [1]shekar.balla@gmail.com, [2]kishan_n@rediffmail.com

Abstract. Free convection heat transfer in a square cavity filled with nanofluid-saturated porous medium with the effects of different nanoparticles in the presence of thermal radiation is investigated in this paper. The top and bottom horizontal walls of cavity are considered adiabatic, while the vertical walls are kept at constant temperatures. The governing partial differential equations are solved by finite element method of Galerkin weighted residual scheme. Numerical results are obtained for different values of the Rayleigh number, radiation parameter and nanofluid volume fraction. The overall investigation of variation of streamlines, isotherms and Nusselt numbers is presented graphically. To examine the accuracy, the present results are compared with the available results.

1. Introduction

Natural convective heat transfer is a significant phenomenon in engineering and industry with widespread applications in diverse fields, such as, geophysics, solar energy, electronic cooling, and nuclear energy. The classical problem of natural convection in square enclosures has many engineering applications such as the cooling systems of electronic components, the building and thermal insulation systems, the built-in-storage solar collectors, the nuclear reactor systems, the food storage industry and the geophysical fluid mechanics.

Low thermal conductivity of conventional heat transfer fluids such as oil, ethylene glycol, and water is a primary restriction in improving the performance and the compactness of many engineering electronic devices. Therefore, there is a strong need to develop advanced heat transfer fluids with substantially higher conductivities. With recently introduced the term of nanofluids by Choi [1], which are the fluids with suspended solid particles of higher thermal conductivity such as metals within it, the need mentioned before has been overcome. The nanofluids have many applications in the industry since materials of nanometer size have unique physical and chemical properties. Convective heat transfer of nanofluids in cavities has been extensively studied by many researchers in recent years. Khanafer et al. [2] investigated the flow and heat transfer performance in a rectangular enclosure using nanofluids for various pertinent parameters and taking into account the solid particle dispersion. Tiwari and Das [3] studied mixed convection in a differentially heated two-sided lid-driven square cavity. One of their conclusions was that nanoparticles were able to change the flow pattern of fluid from natural to forced convection regime. Hence, it is worth it to mention here that all of the above surveyed

works dealt with viscous clear fluids (non-porous media) and that most of them reported that it was not always true that increasing the volume fraction of solid particles enhanced the heat transfer rate. It is found that a relatively a limited papers dealing with nanofluids saturated in porous media were published; and most of these papers studied the boundary layer flow.

Nield and Kuznetov [4] examined the influence of nanoparticles natural convection past a vertical plate. Their analytical study was based on Brownian motion and thermophoresis (for nanofluids) and Darcy model (for porous media). Ahmad and Pop [5] studied numerically mixed convection boundary layer flow using three different nanoparticles based on the conventional model of Tiwari and Das [3] which incorporates only the nanofluid volume fraction. They followed Darcy model also to interpret the flow in porous media. Balla and Naikoti [6] studied free convective heat transfer in fluid saturated porous cavity. Cimpean and Pop [7] studied fully developed steady-state mixed convection flow of nanofluids in a inclined porous channel. A lattice Boltzmann model is developed to simulate the convection heat transfer utilizing Al_2O_3-water nanofluids in a square cavity by He et al. [8]. However, the field of nanofluids saturated in porous cavities is found published in very little works as in Sun and Pop [9] and Chamkha and Ismael [10]. Sun and Pop [9] considered a triangular enclosure heated by a wall heater and filled with a porous medium and saturated with three different nanofluids. A two-dimensional numerical study has been performed by Sheikholeslami et al. [11] to investigate free convection inside a square cavity filled with Cu-water nanofluid. Jou and Tzeng [12] numerically investigated the heat transfer performance of nanofluids inside the two-dimensional rectangular enclosures and found that increasing the volume fraction causes a significant increase in average heat transfer rate. A side heated nanofluid-filled square cavity using a non-homogeneous model has been numerically studied by Celli [13]. Thermal radiation effects are extremely important in the flow processes involving high temperature and controlling heat transfer in industry where heat controlling factors determine the quality of the final product. Thermal radiation has a significant role in the overall surface heat transfer when the convection heat transfer coefficient is small. The influence of radiation on mixed convection from vertical surface in a porous medium was studied by Bakier [14]. The effects of radiation on the thermal boundary layer flow have been considerably researched ([15]-[17]). Zahmatkesh [18] has found that the presence of thermal radiation makes temperature distribution nearly uniform in the vertical sections inside the enclosure and causes the streamlines to be nearly parallel with the vertical walls. Radiation effects on transient natural convection flow of nanofluid has been investigated by Balla and Naikoti [19]. The effect of thermal radiation on boundary layer flow and mass transfer over a moving vertical porous surface has been reported by Makinde [20]. Chiu et al. [21] studied numerically mixed convection and heat transfer inside a horizontal rectangular duct in the presence of thermal radiation. It reveals that radiation effect tends to balance the temperature in the flow at the downstream. It is seen that the bulk temperature development was enhanced with the larger Rayleigh number and smaller conduction-to-radiation parameter.

Recently, Sheremet et al. [22] investigated free convection in a nanofluid-saturated porous square cavity using Tiwari and Das [3] nanofluid model. Thus the motivation of the study is to examine the influence of thermal radiation on natural convection flow field and temperature distribution in a square cavity filled with nanofluid saturated porous medium. In the present study the three types of nanoparticles are considered to analyse the flow and heat transfer characteristics. The numerical results for streamlines, isotherms and average Nusselt number are presented graphically.

2. Mathematical formulation

Consider the free convection in a two-dimensional porous square cavity filled with nanofluid based on water and different type of nanoparticles: Cu, Al_2O_3, TiO_2 in the presence of thermal radiation. A schematic geometry of the problem is shown in figure 1. Let u and v be the

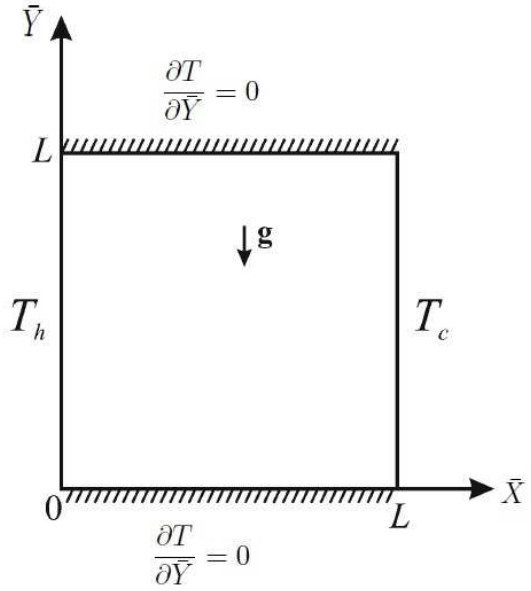

Figure 1. Physical model and coordinate system.

velocity components along $\bar{X}$ and $\bar{Y}$ directions respectively and L is the height of the cavity. It is assumed that the top and bottom walls of the cavity are adiabatic. Also it is assumed that the left wall is the source of heat and maintained at T_h, while the right walls is kept at T_c, where $T_h > T_c$. It is further assumed that the base fluid and the nanoparticles are in thermal equilibrium, the nanofluid is newtonian and incompressible and the flow is laminar. Using the Darcy-Boussinesq approximation $\rho = \rho_0 \left(1 - \beta(T - T_0)\right)$, the basic equations are

$$u = -\frac{K}{\mu_{nf}} \left(\frac{\partial P}{\partial \bar{X}} \right), \tag{1}$$

$$v = -\frac{K}{\mu_{nf}} \left(\frac{\partial P}{\partial \bar{Y}} + \rho_{nf} g \right), \tag{2}$$

$$u \frac{\partial T}{\partial \bar{X}} + v \frac{\partial T}{\partial \bar{Y}} = \alpha_{nf} \left(\frac{\partial^2 T}{\partial \bar{X}^2} + \frac{\partial^2 T}{\partial \bar{Y}^2} \right) - \frac{1}{(\rho C_P)_{nf}} \frac{\partial q_r}{\partial \bar{Y}}. \tag{3}$$

On eliminating the pressure from equations (1) and (2) and using the stream function $\bar{\psi}$ which is defined as $u = \frac{\partial \bar{\psi}}{\partial \bar{Y}}$ and $v = -\frac{\partial \bar{\psi}}{\partial \bar{X}}$ we obtain,

$$\frac{\partial^2 \bar{\psi}}{\partial \bar{X}^2} + \frac{\partial^2 \bar{\psi}}{\partial \bar{Y}^2} = -\frac{gK \left[\phi \rho_p \beta_p + (1 - \phi) \rho_f \beta_f\right]}{\mu_{nf}} \frac{\partial T}{\partial \bar{X}}, \tag{4}$$

where K is the permeability of the porous medium, g is the acceleration due to gravity, p is the pressure, ρ is the density, β is the thermal expansion coefficient, μ is the dynamic viscosity, k is the thermal conductivity and C_p is the specific heat at a constant pressure. The physical properties of the nanofluid are given by

$$\mu_{nf} = \frac{\mu_f}{(1 - \phi)^{2.5}}, \quad (\rho C_p)_{nf} = (1 - \phi)(\rho C_p)_f + \phi (\rho C_p)_p,$$

$$\frac{k_{nf}}{k_f} = \frac{k_p + 2k_f - 2\phi(k_f - k_p)}{k_p + 2k_f + \phi(k_f - k_p)}, \quad (\rho\beta)_{nf} = (1-\phi)(\rho\beta)_f + \phi(\rho\beta)_p.$$

The radiative heat flux term $\frac{\partial q_r}{\partial \bar{Y}}$ in the energy equation is simplified by invoking Rosseland approximation Brewester [27] as follows:

$$q_r = -\frac{4\sigma^*}{3k^*}\frac{\partial T^4}{\partial \bar{Y}}. \tag{5}$$

Equation (5) can be linearized by expanding T^4 into the Taylor series about T_∞. Neglecting higher order terms, we obtain

$$T^4 \simeq 4T_\infty^3 T - 3T_\infty^4. \tag{6}$$

Using equations (5) and (6), We obtain,

$$\frac{\partial q_r}{\partial \bar{Y}} = -\frac{16\sigma^* T_\infty^3}{3k^*}\frac{\partial^2 T}{\partial \bar{Y}^2}. \tag{7}$$

Introducing the following dimensionless variables

$$x = \frac{\bar{X}}{L}, \;\; y = \frac{\bar{Y}}{L}, \;\; \psi = \frac{\bar{\psi}}{\alpha_f}, \;\; \theta = \frac{T - T_c}{T_h - T_c}.$$

The equations (4) and (3) transform to the following form

$$\frac{1}{(1-\phi)^{2.5}}\left(\frac{\partial^2\psi}{\partial x^2} + \frac{\partial^2\psi}{\partial y^2}\right) = -Ra\left[\phi\left(\frac{\rho_p}{\rho_f}\right)\left(\frac{\beta_p}{\beta_f}\right) + (1-\phi)\right]\frac{\partial\theta}{\partial x}, \tag{8}$$

$$\frac{\partial\psi}{\partial y}\frac{\partial\theta}{\partial x} - \frac{\partial\psi}{\partial x}\frac{\partial\theta}{\partial y} = \frac{\alpha_{nf}}{\alpha_f}\left[\frac{\partial^2\theta}{\partial x^2} + \left(1 + \frac{4}{3}R_d\right)\frac{\partial^2\theta}{\partial y^2}\right]. \tag{9}$$

where Ra is the Rayleigh number and R_d is the radiation parameter

$$Ra = \frac{gK\beta_f(T_h - T_c)L}{\nu_f\alpha_f}, \;\; R_d = \frac{4\sigma^* T_\infty^3}{K_{nf}k^*}.$$

The corresponding boundary conditions are

$$\begin{array}{c} \psi = 0, \;\; \theta = \frac{1}{2} \;\; \text{at} \;\; x = 0, \\ \psi = 0, \;\; \theta = -\frac{1}{2} \;\; \text{at} \;\; x = 1, \\ \psi = 0, \;\; \frac{\partial\theta}{\partial y} = 0 \;\; \text{at} \;\; y = 0, 1. \end{array} \tag{10}$$

The physical quantity of interest is the local Nusselt number which is defined as

$$Nu = -\frac{k_{nf}}{k_f}\left(1 + \frac{4}{3}R_d\right)\left(\frac{\partial\theta}{\partial x}\right)_{x=0}.$$

Table 1. Thermo physical properties of base fluid and nanoparticles (Oztop and Abu-Nada [23]).

Physical properties	water	Cu	Al_2O_3	TiO_3
$C_p\ (J/KgK)$	4179	385	765	686.2
$\rho\ (Kg/m^3)$	997.1	8933	3970	4250
$k\ (W/mK)$	0.613	400	40	8.9538
$\alpha \times 10^{-7}\ (m^2/s)$	1.47	1163.1	131.7	30.7
$\beta \times 10^{-5}\ (1/K)$	21	1.67	0.85	0.9

3. Method of solution

The dimensionless partial differential equations (8) and (9) are solved by weighted residual Galerkin finite element method [26]. In weighted residual approach the unknowns are replaced by approximate trial solution which in the context of a discretized domain are given by polynomial relationships to obtain the residuals. These residuals are then multiplied by weight functions and their integrals over an element domain are set to be zero. Let the approximate solutions of ψ, θ are $\psi = \sum_{i=1}^{3} \psi_i \xi_i$; $\theta = \sum_{i=1}^{3} \theta_i \xi_i$; where ξ_i are the linear interpolation functions for a triangular element. The Galerkin finite element model for a typical element Ω_e is given by

$$\begin{bmatrix} [K^{11}] & [K^{12}] \\ [K^{21}] & [K^{22}] \end{bmatrix} \begin{bmatrix} \{\psi\} \\ \{\theta\} \end{bmatrix} = \begin{bmatrix} \{F^1\} \\ \{F^2\} \end{bmatrix},$$

where,

$$K^{11} = \frac{1}{(1-\phi)^{2.5}} \iint_{\Omega_e} \left(-\frac{\partial \xi_j}{\partial x}\frac{\partial \xi_i}{\partial x} - \frac{\partial \xi_j}{\partial y}\frac{\partial \xi_i}{\partial y} \right) dxdy\ ,$$

$$K^{12} = Ra \left[\phi \left(\frac{\rho_p}{\rho_f} \right) \left(\frac{\beta_p}{\beta_f} \right) + (1-\phi) \right] \iint_{\Omega_e} \left(\xi_j \frac{\partial \xi_i}{\partial x} \right) dxdy\ , F^1 = 0\ , K^{21} = 0\ , F^2 = 0\ ,$$

$$K^{22} = \iint_{\Omega_e} \left(\xi_j \frac{\partial \bar{\Psi}}{\partial y}\frac{\partial \xi_i}{\partial x} - \xi_j \frac{\partial \bar{\Psi}}{\partial x}\frac{\partial \xi_i}{\partial y} + \frac{\alpha_{nf}}{\alpha_f}\frac{\partial \xi_j}{\partial x}\frac{\partial \xi_i}{\partial x} + \frac{\alpha_{nf}}{\alpha_f}\left(1 + \frac{4}{3}R_d\right)\frac{\partial \xi_j}{\partial y}\frac{\partial \xi_i}{\partial y} \right) dxdy\ ,$$

where $\bar{\Psi} = \sum_{j=1}^{3} \bar{\Psi}_j \xi_j$. The whole domain is divided into 800 triangular elements of equal size. Each element is three nodded, therefore whole domain contains 441 nodes. Each element matrix is of order 6×6, since at each node two functions are to be evaluated. Hence after assembly of the elemental equations, we obtain a system of 882 non-linear coupled equations. To linearize the system of equations the function $\bar{\Psi}$ is incorporated, which is assumed to be known. After imposing the boundary conditions a matrix of system of linear equations of order 722×722 is remained. This system has been solved by using Gauss seidel iteration method.

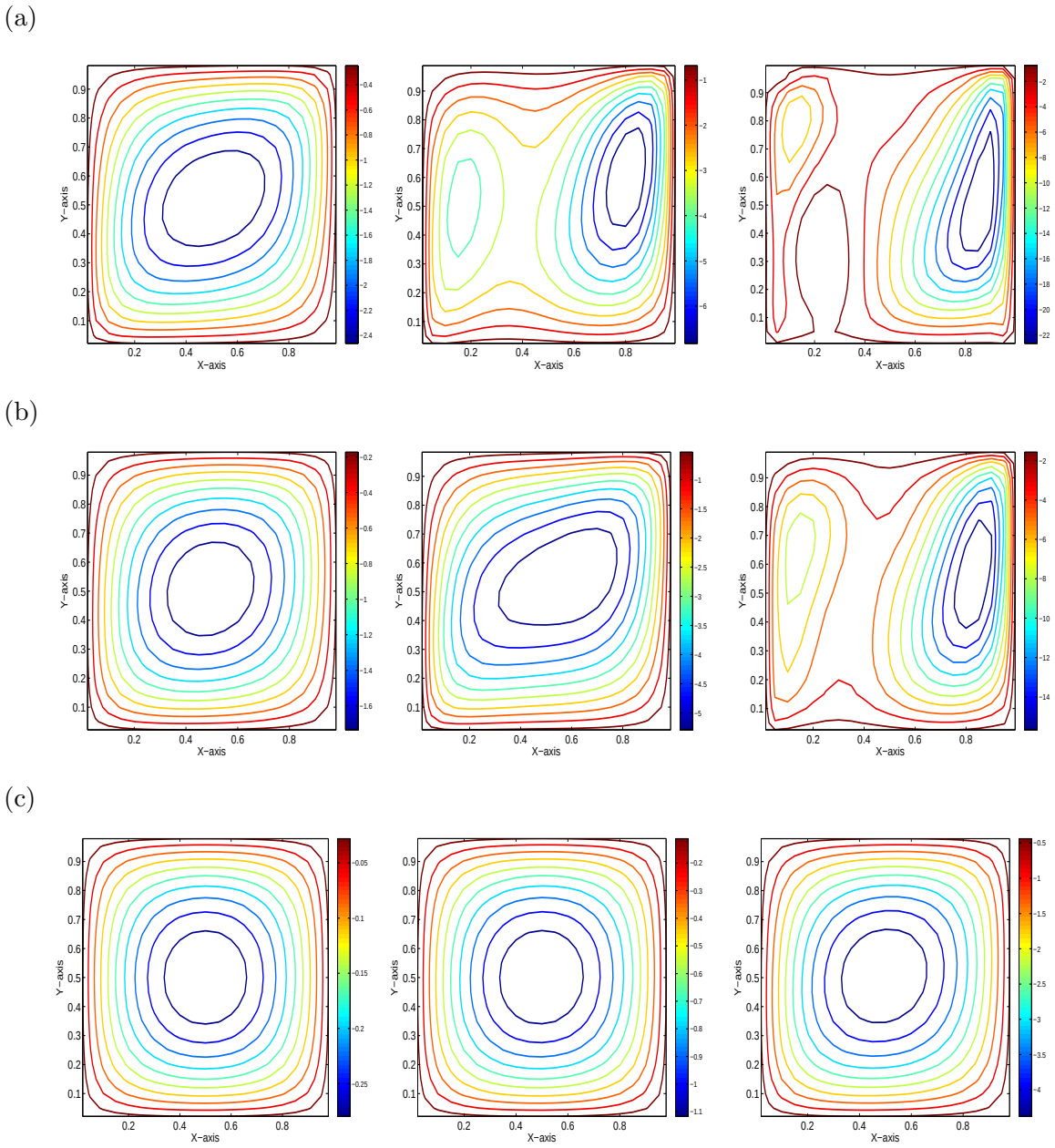

Figure 2. Stream lines for (a) $\phi = 0.02$ (b) $\phi = 0.2$ (c) $\phi = 0.6$ and Ra=50,200,800.

4. Results and discussions

The numerical results are presented by the streamlines, isotherms and local Nusselt number. In the present study the following values have been taken for key parameters: Rayleigh number (Ra=50,200,800), thermal radiation parameter (R_d=0,0.5,1) and the volume fraction of nanofluid (ϕ=0.02,0.2,0.6). The effect of nanoparticle volume fraction ϕ on the flow and heat transfer characteristics has been considered for three types of nanofluids namely Cu, Al_2O_3 and TiO_3. To check the validity of the present method and code, a comparison with selective data from the published work was carried out. The present results are displayed in table 2 for some comparative data with those reported by Manole and Lage [24], Baytas and Pop [25] and Sheremet et al. [22].

Table 2. Comparison of the Nusselt numbers at the hot wall for ϕ=0.

	Ra=10	Ra=100	Ra=1000	Ra=10000
Manole and Lage [24]		3.118	13.637	48.117
Baytas and Pop [25]	1.079	3.16	14.06	48.33
Sheremet et al. [22]	1.079	3.115	13.667	48.823
Present results	1.08	3.129	13.7353	48.5451

The mechanism of forming such streamlines is as follows: the fluid near the left hot wall (interface) is heated, and then it moves to the right cold wall (due to differentially heating) and moves up due to convection (Buoyancy force). When it becomes closer to the upper adiabatic wall, it turns to the right and falls down to the lower adiabatic wall. Hence, a single vortex of clockwise rotation (negative sign) is formed within the porous domain. Figure 2 displays the streamlines for different values of the Rayleigh number Ra=50,200,800 and for copper nanoparticles with different values of volume fractions ϕ=0.02,0.2,0.6. From the figure it can be observed that when the Rayleigh number Ra increases, the flow convection is strengthened, the flow cell is extended along the vertical axis and the boundary layers become more significant. Depending on the Ra and ϕ single or multiple cell convection was found. Further it can be noticed that for large value of Rayleigh number (Ra=800), the convection mode is pronounced, the flow region in the cavity split into two cells. From the figure it is also revealed that the strength of the streamlines decreases with the increase of nanoparticle volume fraction ϕ. It is interestingly noticed that the influence of ϕ is predominating for the higher Ra values and it is meager for lower values of Ra. In case of $\phi = 0.6$, for different values of Ra the convection is dominant, the circulation cell is very stronger and it is in the centre of the cavity.

Figure 3 illustrates the isotherms for different values of Ra=50,200,800 for copper nanoparticles with volume fractions ϕ=0.02,0.2,0.6. For low Rayleigh number Ra=50, the conduction raising is dominant which defines weak heat transfer. It can be seen from the figure that the isotherms are vertically stratified. As the Rayleigh number Ra increases the convection is dominant and the isotherms become denser along the vertical walls. Thus Rayleigh number helps in minimizing the conduction heat transfer and increasing the convection heat transfer. The isotherms become parallel to hot wall with the increase in the nanopartical volume fraction ϕ, indicating weak heat transfer. However, the effect of Rayleigh number on heat transfer increases with the lower values of ϕ.

Figures 4 and 5 illustrate the effect of Rayleigh number Ra on streamlines and isotherms respectively, for three types of nanoparticles Cu, Al_2O_3, TiO_3 with nanoparticle volume fraction ϕ=0.2. From figure 4 it is observed that for Ra=50 a vortex with clock wise rotation is formed. The vortex is elongated in horizontal direction and further split into two vortices as Ra is increased to 800 in case of Cu. The flow pattern is nearly same as that of Cu, but with the change in the flow intensity for the nanofluids Al_2O_3, TiO_3. It is also observed that the circulation strength is higher for Cu and it is lower for Al_2O_3 regardless of the Rayleigh number. From figure 5 it is observed that, for the nanofluid Cu, the isotherms change almost from vertical lines to horizontal lines in the central region of the cavity as Ra increases from 50 to 800. For higher values of Ra the isotherms are closer near the vertical walls. The increase in the Rayleigh number Ra enhances the rate of heat transfer. Similar pattern of isotherms is observed for the nanofluids Al_2O_3, TiO_3 except the values of isotherms. It is also observed that Cu has higher isotherm value than the other nanofluids.

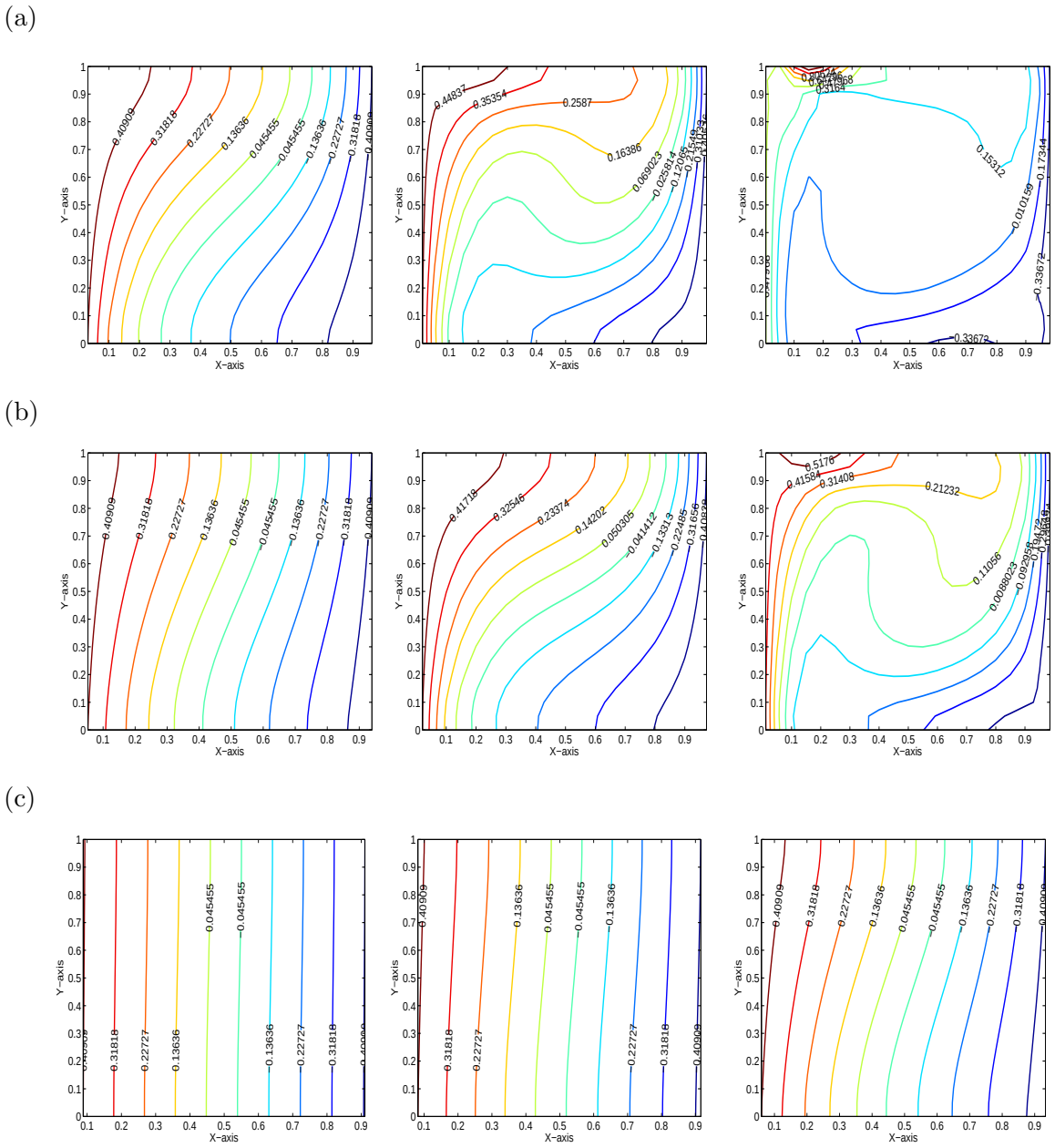

Figure 3. Isotherms for (a) $\phi = 0.02$ (b) $\phi = 0.2$ (c) $\phi = 0.6$ and Ra=50,200,800.

The effect of nanoparticle volume fraction ϕ on the behaviour of streamlines is presented for the radiation parameter R_d=0,0.5,1 in figure 6. Due to heating of the left wall the fluid rises towards the cold wall. From the figure 6(a) it is observed that the streamlines in the cavity form in to two cells for ϕ=0.02. The effect of radiation parameter is to strengthen the flow intensity. For ϕ=0.2, one flow cell is formed and elongated horizontally. As R_d increases, the circulation strength enhances. A centrally circulated cell is appeared in case of ϕ=0.6 and its strength increases with the increase in the radiation parameter. Figure 7 depicts the effect of radiation parameter R_d on isotherms for different volume fractions of nanofluid ϕ=0.02,0.2,0.6. The thermal radiation significantly alters the wall temperature and generates thermal instabilities while reducing the overall heat transfer rates. The effect of R_d is to reduce the heat transfer for

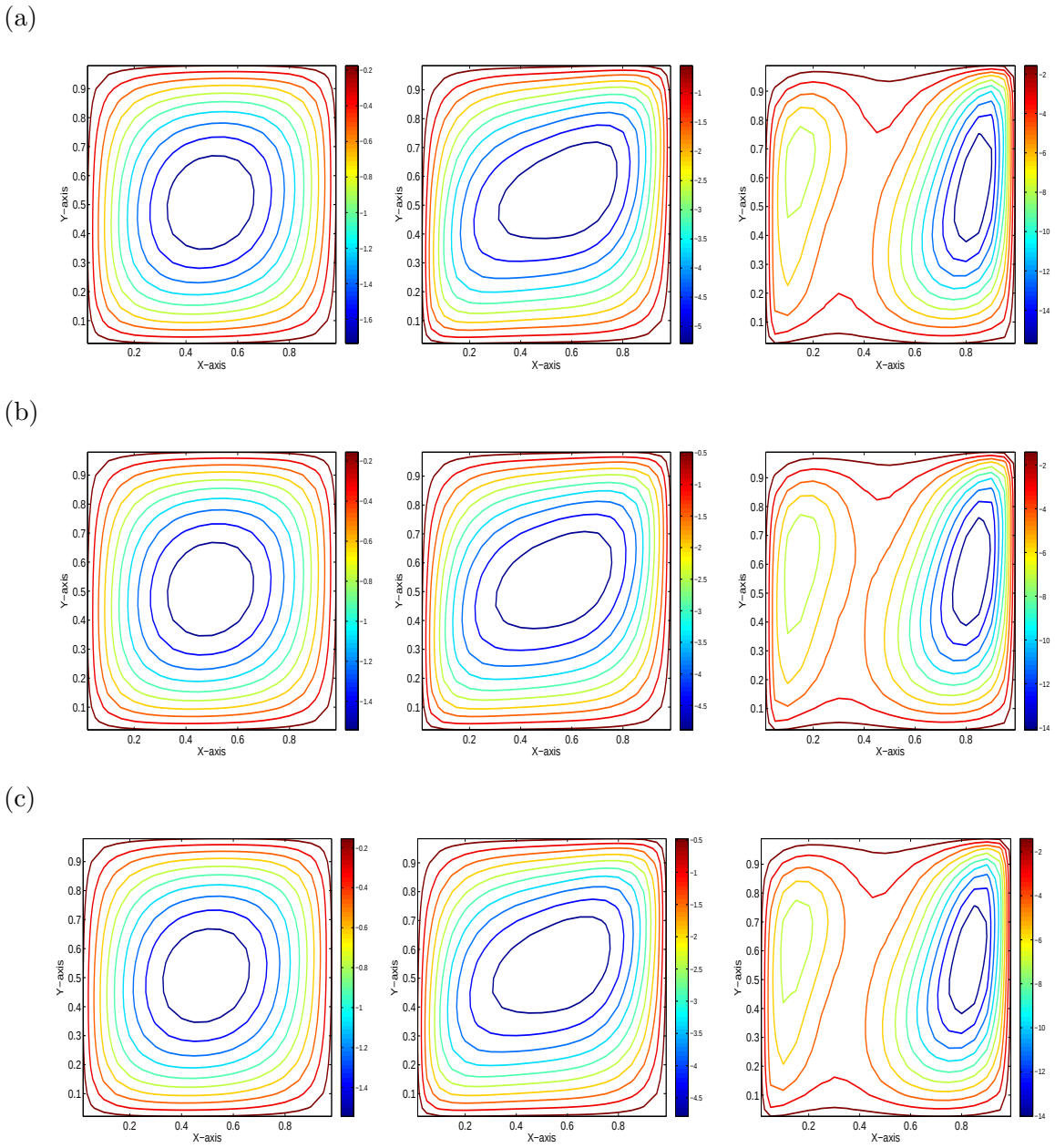

Figure 4. Stream lines for (a) Cu (b) Al_2O_3 (c) TiO_3 and Ra=50,200,800.

lower values of ϕ. As the value of ϕ increases the effect of radiation parameter is less.

Figures 8-11 present the distribution of local Nusselt number Nu along the hot vertical wall ($x = 0$) for different values of ϕ, Ra, R_d and for the three nanofluids Cu, Al_2O_3, TiO_3. Figure 8 shows a linear variation of the local Nusselt number with the nanoparticle volume fraction. Moreover, an increase in ϕ leads to decrease the local Nusselt number near the bottom wall and the opposite phenomena is noticed at the top wall. Figure 9 depicts that as the Rayleigh number Ra increases, the local Nusselt number also increases near bottom wall $y = 0$, and the variation is less at the top wall. From the figure 10, it can be observed that the influence of radiation parameter on Nusselt number leads to increase the local Nusselt number. Figure 11 reveals that the local Nusselt number value decreases when the nanofluid changes in the order

(a)

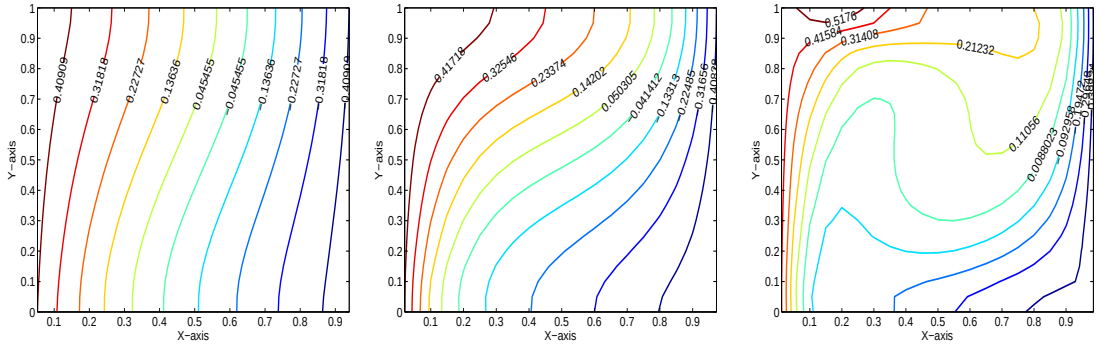

(b)

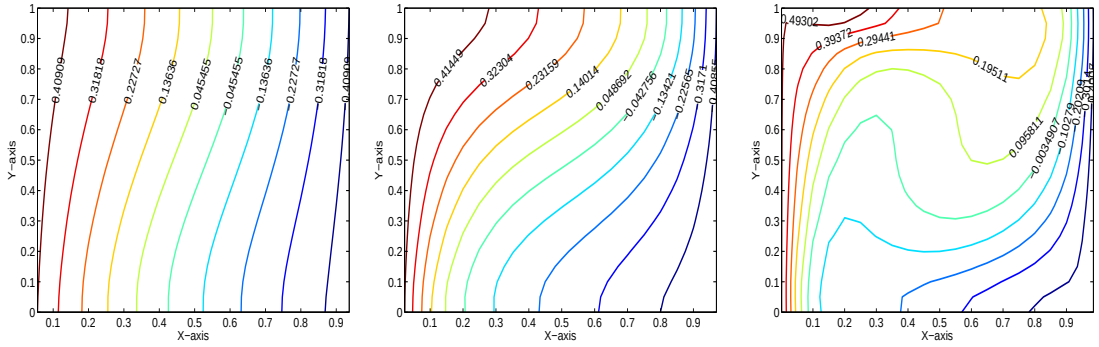

(c)

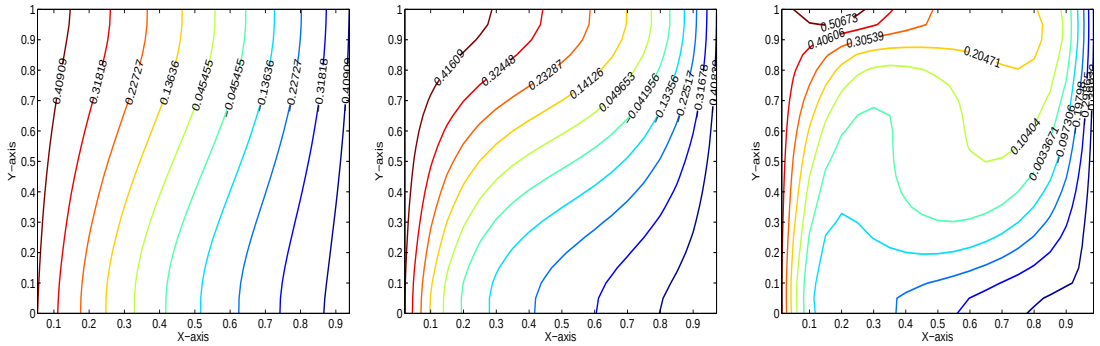

Figure 5. Isotherms for (a) Cu (b) Al_2O_3 (c) TiO_3 and Ra=50,200,800.

as Cu, TiO_3, Al_2O_3.

5. Conclusion

Natural convection flow and heat transfer in a porous square cavity filled with nanofluid under the influence of thermal radiation is studied. The flow and temperature fields as well as heat transfer rate are analysed for various values of flow parameters such as Rayleigh number Ra, nanoparticle volume fraction ϕ and radiation parameter R_d. The computational results lead to the following conclusions:

- The flow pattern takes single or double cell form depending on Ra and ϕ. The flow circulation is pronounced with higher values of Ra and ϕ. The heat transfer increases

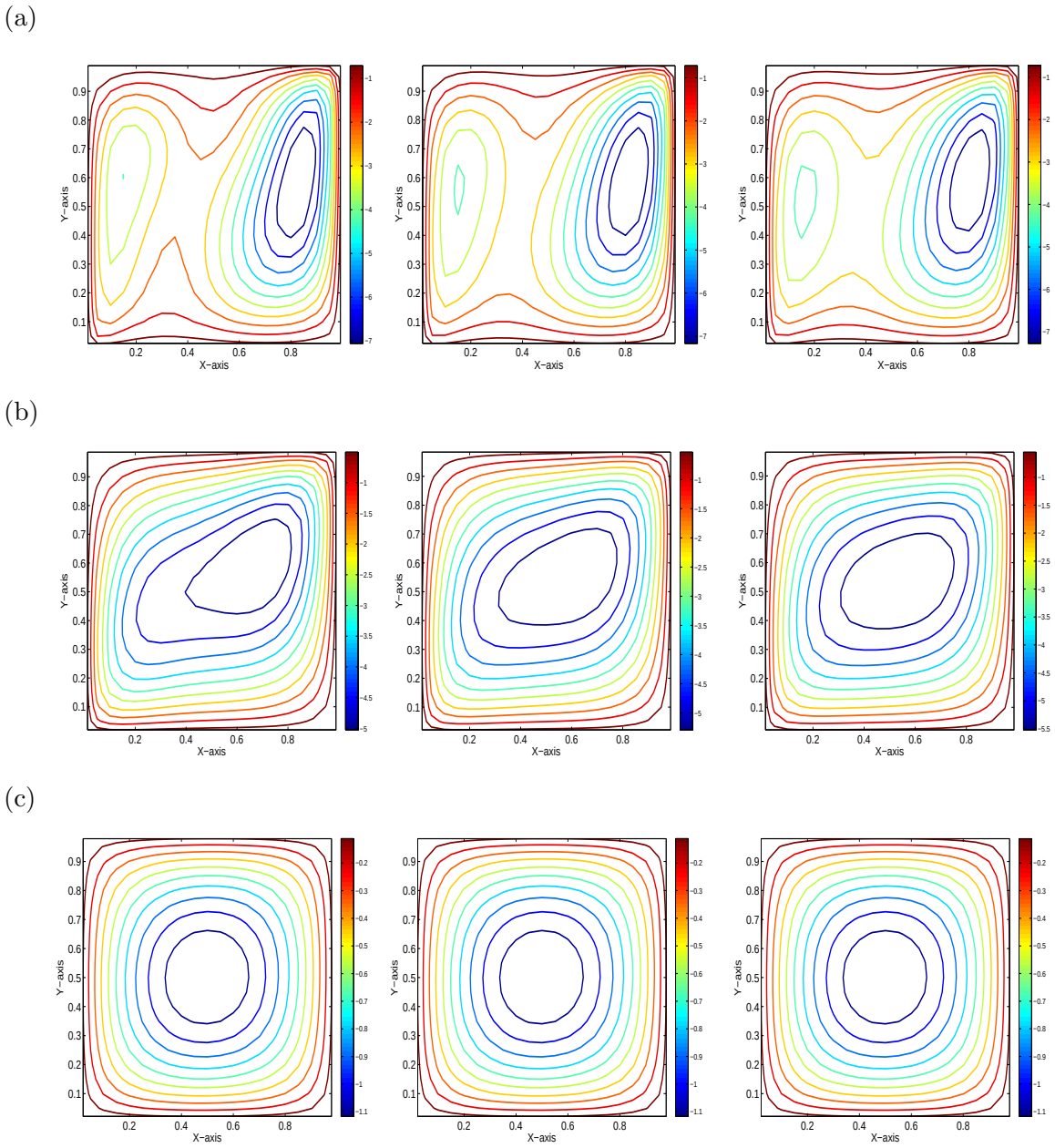

Figure 6. Streamlines for (a) $\phi = 0.02$ (b) $\phi = 0.2$ (c) $\phi = 0.6$ and R_d=0,0.5,1.

with the increase in Ra, while decreases with the increase in ϕ.

- The strength of the flow increases with the increase in the radiation parameter R_d. The effect of R_d leads to reduce the isotherm values.
- The heat transfer and flow intensity are higher for the nanoparticles Cu while they are lower for Al_2O_3.
- The Nusselt number is increase with the increase in radiation parameter R_d and Rayleigh number Ra, while it decreases with the increase in nanoparticle volume fraction ϕ. Further, it decreases when the nanofluid changes in the order as Cu, TiO_3 and Al_2O_3.

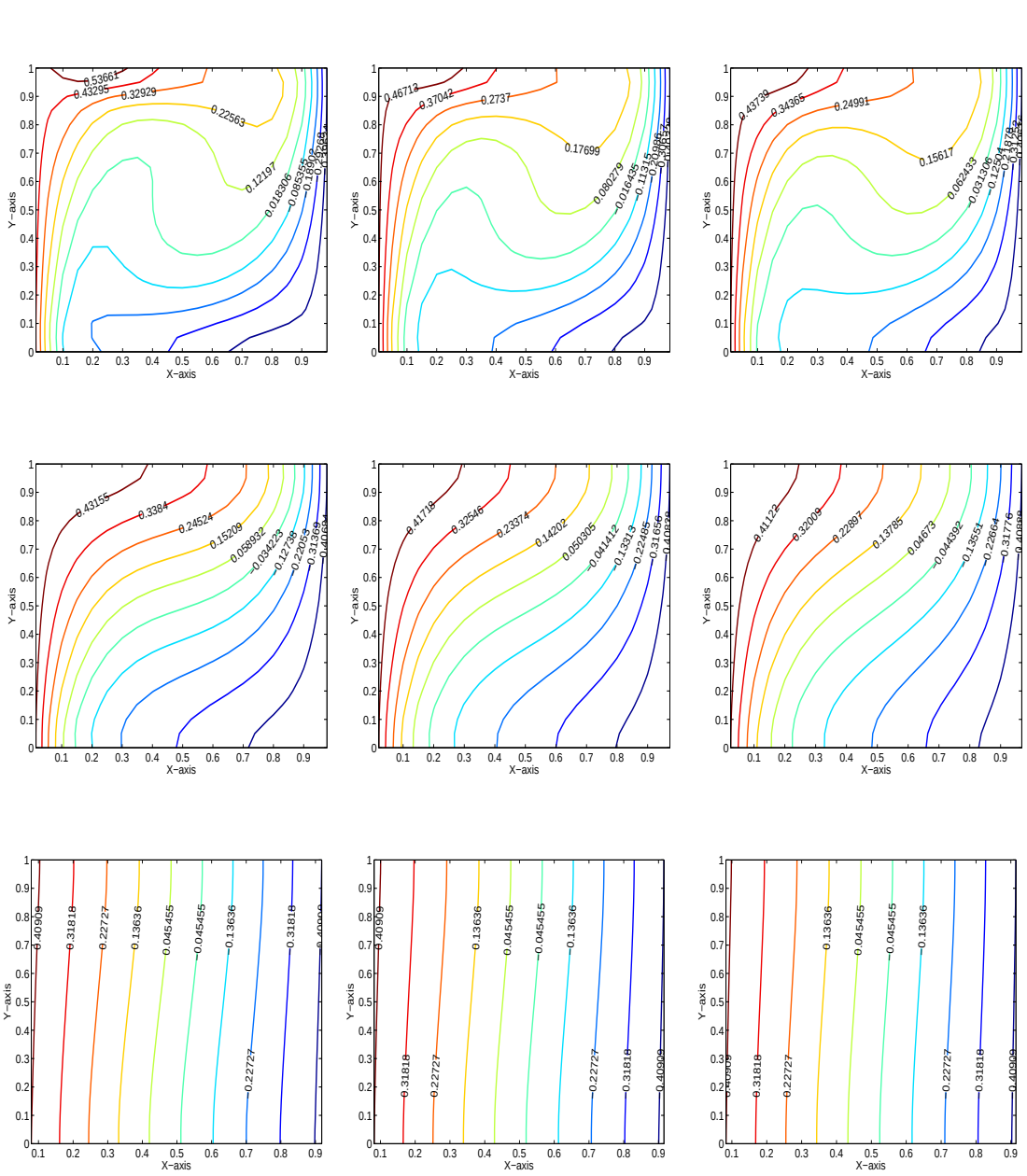

Figure 7. Isotherms for (a) $\phi = 0.02$ (b) $\phi = 0.2$ (c) $\phi = 0.6$ and R_d=0,0.5,1.

References

[1] Choi S U S 1995 Enhancing thermal conductivity of fluids with nanoparticles *Proceedings of the 1995 ASME International Mechanical Engineering Congress and Exposition* vol 66 (San Francisco, USA: ASME, FED 231/MD) 99-105

[2] Khanafer K, Vafai K and Lightstone M 2003 Buoyancy-driven heat transfer enhancement in a two-dimensional enclosure utilizing nanofluids *Int. J. Heat Transf.* **46** 3639-53

[3] Tiwari R K and Das M K 2007 Heat transfer augmentation in a two-sided lid-driven differentially heated square cavity utilizing nanofluids *Int. J. Heat Mass Transfer.* **50** 2002-18

[4] Nield D A and Kuznetsov A V 2009 The ChengMinkowycz problem for natural convective boundary-layer flow in a porous medium saturated by a nanofluid *Int. J. Heat Mass Transfer.* **52** 5792-95

[5] Ahmad S and Pop I 2010 Mixed convection boundary layer flow from a vertical flat plate embedded in a porous medium filled with nanofluids *Int. Commun. Heat Mass Transfer.* **37** 987-91

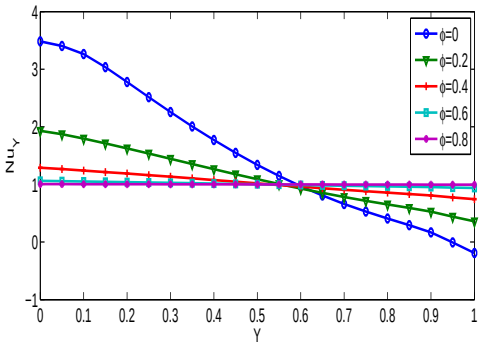

Figure 8. Effect of nanoparticle volume fraction ϕ on Nusselt number.

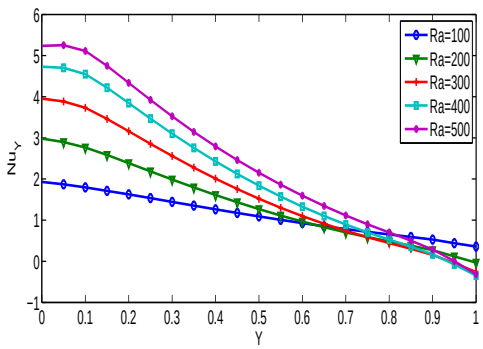

Figure 9. Effect of Rayleigh Ra on Nusselt number.

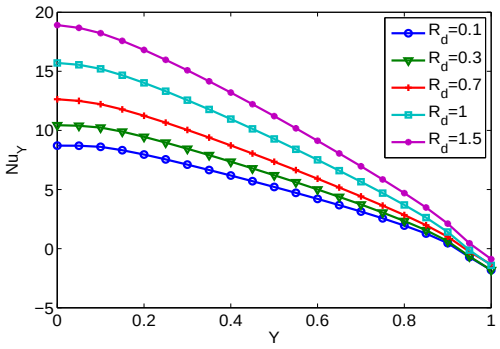

Figure 10. Effect of radiation parameter R_d on Nusselt number.

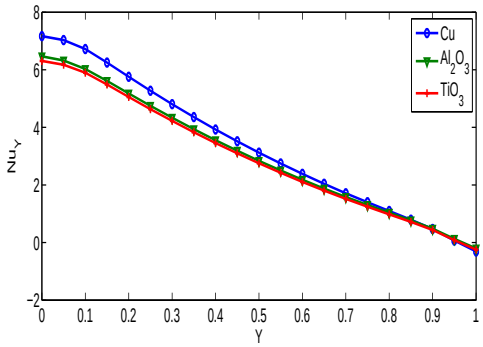

Figure 11. Effect of nanofluid on Nusselt number.

[6] Balla C S and Naikoti K 2015 Soret and Dufour effects on free convective heat and solute transfer in fluid saturated inclined porous cavity *Engineering Science and Technology, an International Journal* **18(4)** 543-54
[7] Cimpean D S and Pop I 2012 Fully developed mixed convection flow of a nanofluid through an inclined channel filled with a porous medium *Int. J. Heat Mass Transfer.* **55** 907-14
[8] He Y, Qi C, Hu Y, Qin B, Li F and Ding Y 2011 Lattice Boltzmann simulation of alumina-water nanofluid in a square cavity *Nanoscale Research Letters* **6** 184
[9] Sun Q and Pop I 2011 Free convection in a triangle cavity filled with a porous medium saturated with nanofluids with flush mounted heater on the wall *Int. J. Thermal Sci.* **50** 2141-53
[10] Chamkha A J and Ismael M A 2013 Conjugate heat transfer in a porous cavity filled with nanofluids and heated by a triangular thick wall *Int. J. Therm. Sci.* **67** 135-51
[11] Sheikholeslami M, Gorji-Bandpy M, Seyyedi S M, Ganji D D, Houman B R and Soheil S 2013 Application of LBM in simulation of natural convection in a nanofluid filled square cavity with curve boundaries *Powder Technology* **247** 87-94
[12] Jou R Y and Tzeng S C 2006 Numerical research of nature convective heat transfer enhancement filled with nanofluids in rectangular enclosures *Int. Commun. Heat Mass Transfer.* **33** 727-36
[13] Celli M 2013 Non-homogeneous model for a side heated square cavity filled with a nanofluid *Int. J. Heat Fluid Flow.* **44** 327-55
[14] Bakier A Y 2001 Thermal radiation effect on mixed convection from vertical surface in saturated porous media *Int. Commun. Heat Mass Transf.* **28** 119-26
[15] Cortell R 2008 Effects of viscous dissipation and radiation on the thermal boundary layer over a nonlinearly stretching sheet *Phys. Lett.* A **372** 631-36
[16] Govardhan K, Kishan N and Balaswamy B 2012 Effect of viscous dissipation and radiation on MHD gas flow and heat and mass transfer over a stretching surface with a uniform free stream *Journal of Engineering*

Physics and Thermophysics **85** 909-16
[17] Naikoti K and Vadithya M 2014 Thermal radiation effects on magneto hydro dynamic flow and heat transfer in a channel with porous walls of different permeability *Thermal Science* **18(suppl.2)** 563-72
[18] Zahmatkesh I 2007 Influence of thermal radiation on free convection inside a porous enclosure *Emir. J. Eng. Res.* **12(2)** 47-52
[19] Balla C S and Naikoti K 2014 Finite element analysis of magnetohydrodynamic transient free convection flow of nanofluid over a vertical cone with thermal radiation *Proceedings of Institution of Mechanical Engineers Part N: Journal of Nanoengineering and Nanosystems* DOI: 10.1177/1740349914552879.
[20] Makinde O D 2005 Free-convection flow with thermal radiation and mass transfer past a moving vertical porous plate *Int. Commun. Heat Mass Transfer.* **32** 1411-19
[21] Chiu H C, Jang J H and Yan W M 2007 Mixed Convection Heat Transfer in Horizontal Rectangular Ducts with Radiation Effects *Int. J. of Heat Mass Transfer.* **50** 2874-82
[22] Sheremet M A, Grosan T and Pop I 2015 Free convection in a square cavity filled with a porous medium saturated by nanofluid using Tiwari and Das' nanofluid model *Transp. Porous Med.* **106** 595-610
[23] Oztop H F and Abu-Nada E 2008 Numerical study of natural convection in partially heated rectangular enclosures filled with nanofluids *International Journal of Heat and Fluid Flow* **29** 1326-36
[24] Manole D M and Lage J L 1992 Numerical benchmark results for natural convection in a porous medium cavity *Heat and Mass Transfer Porous Media* **105** 44-59
[25] Baytas A C and Pop I 1999 Free convection in oblique enclosures filled with a porous medium *Int. J. Heat Mass Transf.* **42** 1047-57
[26] Reddy J N 1984 *An introduction to the finite element method* (New York: Mc Graw-Hill)
[27] Brewester M Q 1992 *Thermal Radiative Transfer and Properties* (New York: John Wiley and Sons)